Effectiveness of Non-penetrating Electroporation Applicators to Function as Impedance Spectroscopy Electrodes

Richard J. Connolly[1,3], Jose I. Rey[1,3], Mark J. Jaroszeski[1,3], Andrew M. Hoff[2,3], Richard Gilbert[1,3] and J. Anthony Llewellyn[1,3]

[1]Department of Chemical & Biomedical Engineering
[2]Department of Electrical Engineering
[3]Center for Molecular Delivery
University of South Florida
4202 East Fowler Avenue
Tampa, FL 33620, USA

ABSTRACT

Electroporation is commonly performed to deliver drugs and genes to cells comprising tissues. A possible way to control and confirm delivery is through the use of impedance spectroscopy. Ideally, this tool should not interfere with delivery and should incorporate the use of electrodes, applicators, used for delivery. This work examines impedance spectra obtained with non-penetrating surface applicators commonly used for skin electroporation. After collecting and processing over 9,000 spectra from three animal models it was determined that the electrode systems tested would have no significant effect on the obtained spectra. Therefore, electroporation applicators currently in use could be used concurrently for the collection of impedance spectra.

Index Terms — **Impedance measurement, impedance spectroscopy, bioelectric-phenomena, biomembranes, electroporation, electropermeabilization, electrodes.**

1 INTRODUCTION

ELECTRIC field mediated plasmid delivery has been demonstrated to be an effective and safe way to achieve gene expression in many animal models [1-5] and recently in the clinic [6]. Skin and skin cancers are specifically promising as targets for DNA delivery [7]. However, the development and optimal use of electric field based (electroporation) delivery protocols in a particular tissue requires initial investigation, characterization and then selection of the appropriate electroporation parameters. This parameter set is reflective of the tissue target, the desired gene expression level and duration, and the collection of electroporation conditions [8].

The collection of electroporation conditions used to deliver DNA and subsequently obtain expression has been termed the electroporation signature [9]. This designation only refers to the properties of the pulsed electricity used to deliver the DNA. This includes the electric field strength, number of pulses, pulse duration and time between pulses. The electroporation signature in no way characterizes the target tissue. Unfortunately, the electroporation signature and the tissue characterization parameters can not be completely decoupled because electrical treatment alters the tissue. This coupling is mingled with the design and geometry of the electrode/applicator system used to apply the pulsed fields. Electrodes with small radii or sharper edges will produce higher field gradients that directly impact gene delivery efficiency while electrodes with wider spacing allow for treatment of larger tissue volumes but require application of higher voltages to achieve desired field strengths. The relationship between the type of applicator and its geometry to the tissue and tissue volume are not well understood.

One means of characterizing the effects of applying electroporation pulses to a particular tissue with a particular applicator is by measuring electrical impedance. Untreated tissue measurements may be of value to determine tissue characteristics and eventually select electroporation parameters that will lead to success. Post electroporation impedance data may be useful to confirm that the tissue has been adequately treated. Finally, impedance data taken during electroporation may be useful as a control or feedback parameter to gauge the amount of electrical treatment necessary. In the preclinical arena, this impedance signature could lead to better understanding and subsequent models of the tissue response to the mediating electric field. However, any impedance measurement system must consider the practical issues involved with eventual clinical application. These considerations relate to safe and convenient operation. One way

Manuscript received on 3 February 2009, in final form 18 July 2009.

of achieving this is to utilize the electrodes used for electroporation to also measure impedance [2, 10].

Skin is a notoriously difficult target for impedance measurements. The difficulty arises from its complex geometry and time dependent physiological processes induced by the measurement system's contact [11]. From a geometry perspective, its structure involves various layers, several junction types, shunts from sweat and sebaceous glands and invaginations associated with hairs. The low frequency impedance contribution (roughly below 10 kHz) is dominated by the stratum corneum (SC). This layer has thickness varying from 6 to 40 μm, depending on the location, and the tissue has the ability to change its hydration according to external and internal stimuli [12]. The relative contributions of the SC layer in viable skin have been assessed experimentally and equivalent circuit models have been developed to describe the mechanisms of skin function. However, the measurement system electrodes themselves may elicit physiological tissue alterations when they come in contact with skin [13].

The aim of this work is to identify impedance signatures which are easily obtained and robust when varying candidate electrode configurations are used *in vivo*. Such an investigation attempts to avoid meeting the severe requirements of systems to be used in constructing theory based models leading to a deeper understanding of the complex fundamental mechanisms involved in tissues. Our expectations include a requirement for rapid measurements to reduce electrode contact induced skin changes and multiple observations to examine the effects of removing and replacing electrodes. The current protocols for electroporation involve preparation of the target tissue site, injection of suspension/solution of the drug or gene constructs and then the actual electroporation, usually with a hand held electrode array. These actions add the expectation that impedance measurements before and after injection and post electroporation would be required. We have used simple electrode systems in order to evaluate what may be obtained to develop a data driven model for monitoring electroporation.

A four stage process was envisaged for the development of a measurement system to obtain an impedance signature which has a quantitative capability of characterizing electroporated tissue. First, measurements designed to yield a description of the initial state of the target tissue using various applicator geometries and configurations are needed to provide a baseline data for untreated tissue. Measurement reproducibility needs to be established for spectra obtained from the same target tissue and from different subjects. In addition, the impact of the measurement process on the target tissue when the applicator is removed, rotated, and then replaced on the skin or moved to different sites must be established. Second, although impedance spectroscopy provides a direct way to examine changes in the target tissue, the data can not be directly used as a tissue characterization tool or as a feedback signal to alter the nature of the applied electric fields when multiple pulses are used for electroporation. Thus, feature extraction techniques must be applied to develop a quantitatively useful signature from the impedance spectra. Third, since current clinical trial electroporation practices involve an injection of a drug or a plasmid, measurements using a similar set of measurement procedures designed to characterize the post-injection tissue must be addressed. Finally, the removal of the electroporating electric field does not stop transport of the drug or gene encoded plasmid across the cell membrane. Optimal clinical application of electroporation requires knowledge of the effectiveness and time history following electroporation. Therefore, an additional set of measurements must be collected to characterize the post-electroporation tissue. These issues place constraints on the nature of the impedance measuring system.

As would be expected, the significance of this systemic examination of the impedance of tissue rests in the determination of the consistence in the behavior of tissue before, during and after electroporation. If the success of an electroporation event could be reliably foreshadowed or monitored optional transport conditions for gene transport in cells should be possible. This paper reports on the first and second stages of the development process for this impedance monitor system process.

2 METHODS

Impedance spectroscopy was performed using a CythorLab (Aditus Medical, Lund, Sweden) Fourier transform impedance monitor [14]. This instrument allows a spectrum to be acquired every 4 s. We used the measurement data for set of n spectra assembled as a 16,382 row by 2n column matrix with alternating columns of real and imaginary quantities and each row representing a spectrum data point.

Low frequency impedance spectra signature data is limited by the duration and nature of the measurement input pulse and the physical influence of the SC. The impedance measurement response spectral signatures of interest are related to an electroporation event and reflect alternations that occur in the deeper layers of the skin. Thus, observed spectra were trimmed to an interval between 0.1 kHz and 125 kHz to produce impedance response signatures. These spectra were taken using different non-penetrating applicator geometries and/or configurations that are currently used in animal models.

Two configurations of a non-penetrating nub array applicator were used to couple the target tissue to the CythorLab system. One applicator had eight 0.7 mm diameter hemispherical-shaped gold plated nub, flat tipped, electrodes arranged as two columns of four electrodes. These flat ended circular rod electrodes were 2 mm between centers and 6 mm between each of the 4 rows. The other consists of four columns of four 0.7 mm diameter hemispherical-shaped gold plated nub electrodes. Each of the sixteen electrodes was 3.5 mm between centers. For the impedance measurements using the 16 nub array the outer two columns were connected to different terminals of the CythorLab system and the inner columns were left electrically floating. This configuration created a separation gap of 9.8 mm between the centers of the sensing electrodes. The 8 electrode array arrangement had the separate 4 nub electrode columns connected to a different terminal in the CythorLab system to create a gap of 2.8 mm between the two sensing columns of electrodes.

Various applicator configurations employed in this study were dictated by their use in clinical trials. In such situations, nubs not involved in the configuration were left unconnected. Although the treatment applied electric field is influenced by these unconnected electrodes, there is no impact on the impedance values as determined from the measurement current after the electroporation pulse has been removed.

Two paired electrode configurations were used. In the first, the applicator consisted of two parallel stainless steel plate electrodes mounted onto the jaws of a Vernier caliper [15, 16]. The caliper allowed the 2 cm by 2 cm plates to pinch a repeatable thickness skin fold when obtaining the impedance spectra. In the second situations, a coaxial applicator was also used to collect impedance data. Its configuration consisted of two concentric circular electrodes that were placed in contact with the surface of the skin. The solid inner electrode had a diameter of 3.2 mm and the outer electrode diameter was 9 mm. The outside wall thickness was 0.4 mm.

Impedance measurements were made on tissue located on the freshly shaven flanks of three different animal models. The first was a Sprague-Dawley rat model (Harlan, Indianapolis, IN), which permitted two sites, #1 and #2, on the right flank of the animal and two sites, #3 and #4, on the left flank of the animal. The second animal model used was C57BL/6 mice (NCI, Frederick, MD), which allowed for data acquisition on the right, site #5, and left, site #6, flanks of the animal. The animal model used in the later phases of these studies was Dunkin-Hartley guinea pigs (Charles River, Wilmington, MA), which also allowed two right flank sites, #7 and #8 and two left flank sites, #9 and #10, for data collection. Multiple impedance measurements were conducted with all combinations of models, sites and applicators. Results presented are typical of the spectra collected and analyzed.

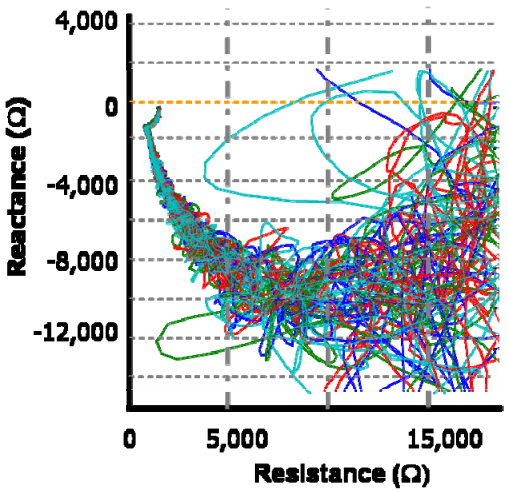

(a)

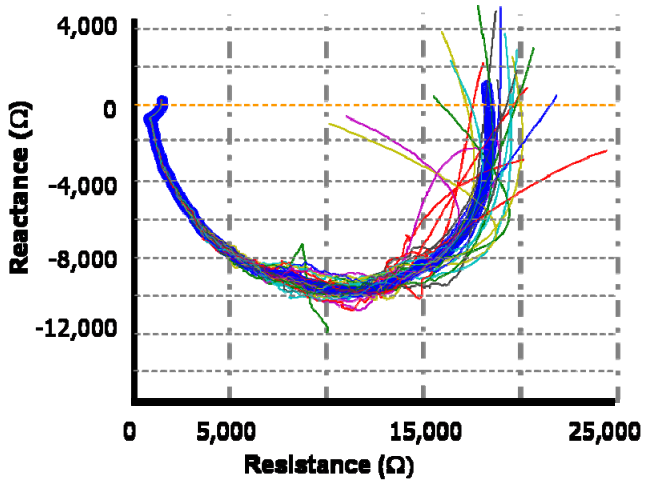

(b)

Figure 1. 24 impedance spectra acquired 4 s apart from the same tissue location. (a) Spectra of rat tissue prior to any data smoothing activity. Impedance data corresponding to resistance values greater than 19,000 Ohm exist but not shown. (b) Savitzky-Golay smoothed plots of all 24 impedance spectra using the shown and not shown impedance data from (a). Reactance values above 4,000 Ohms not shown to scale.

3 Results and Disscussion

The merit of employing impedance spectroscopy to monitor an electroporation process is dependent on the ability to make the measurements without intruding on the process itself. Figure 1a indicates that the noise in the data is a preliminary challenge that must be addressed before the intrusive nature of impedance spectroscopy may be assessed. It is a representative plot of the raw spectral data for 24 impedance spectra with impedance components, resistance, as x-axis values and corresponding imaginary components, reactance, as y-axis values. In this specific case, spectra were obtained using the 8 electrode array at intervals of 4 s on the flank of a Sprague-Dawley rat model. This Nyquist style plot presents the impedance information for lower frequencies toward the right side of the graph. However, it does not present negative imaginary component values on the upper section of the y-axis as is often the practice in electrochemically oriented discussions; our focus is on the basic form of the impedance signal rather than on an electrochemical analysis. The plot represents a behavior illustration of the impedance observations.

Inspection of Figure 1a illustrates that the collected spectra were extremely noisy. This was "normal" measurement noise plus accompanying major excursions which were attributed to the use of surface electrodes for *in vivo* measurements. The effect of Savitzky-Golay quadratic smoothing with a frame size of 501 points on the raw spectra presented in Figure 1a is shown in Figure 1b. This frame size was chosen to preserve possible small features and does not completely remove the occasional large excursions which occur with *in vivo* environments. These features were retained to assess their effects on the subsequent data analysis. As might be anticipated from visual inspection of Figure 1a, the lower frequency ranges showed the greatest excursions in the smoothed spectra. With this smoothing method in hand, the raw and smoothed spectra were examined for systematic (non-random) differences, using runs analysis and visual examination of histograms of the differences between raw and smoothed data. The objective was to determine if the measurement current altered the tissue with respect to time,

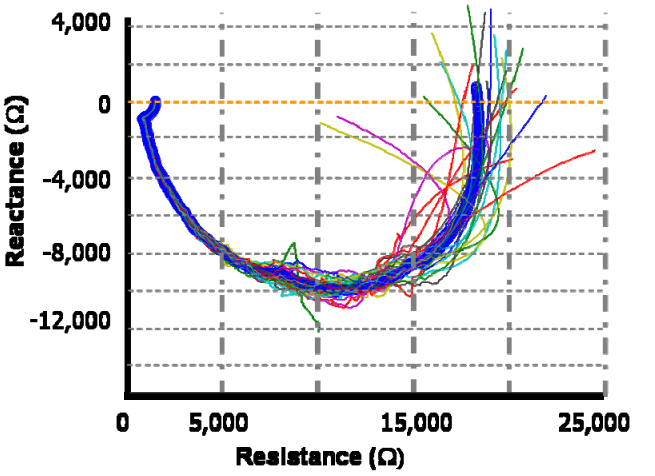

(a)

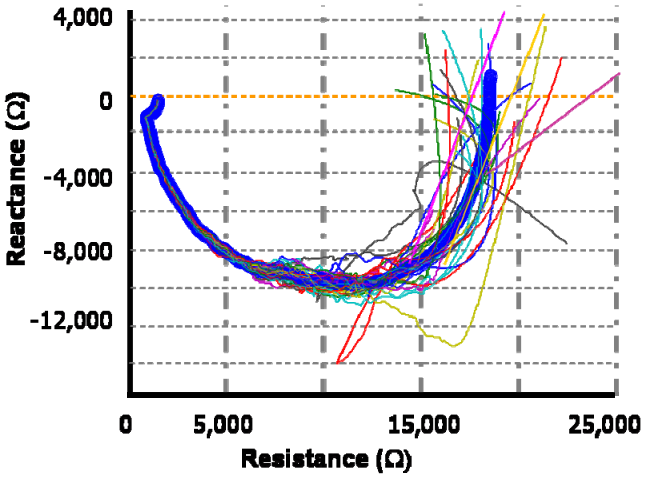

(b)

Figure 2. 24 impedance spectra acquired from two different tissue locations on the same Sprague-Dawley rate. (a) Savitzky-Golay smoothed version of impedance spectra at site1but without applicator rotation. (b) Savitzky-Golay smoothed spectra with applicator rotated through 5 angles (0°, 45°, 90°, 135°, and 180°) with 4 spectra taken at each angle followed by a repeat 4 spectra set acquisition at 90.

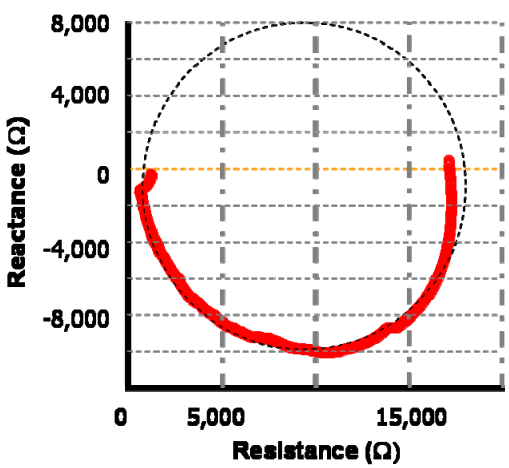

(a)

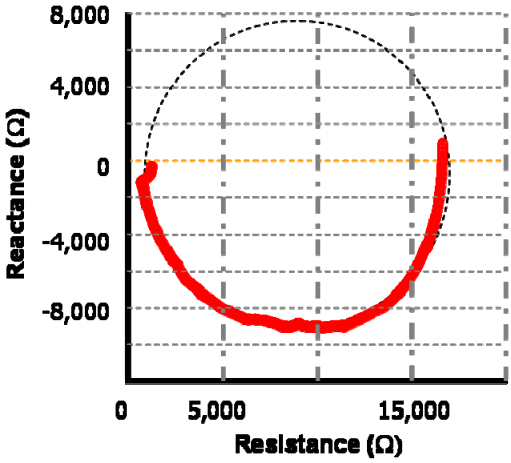

(b)

Figure 3. Model fit for the 24 spectra taken at two different tissue locations on different Sprague-Dawley rats. Plots representative of all measurement experiments with any applicator (a) model fit for average spectra of site location, site 1, on right flank of animal (b) model fit for average spectra of site location, site 3, on left flank of animal.

tissue site, electrode geometry, removal and replacement, and subject variation.

The Savitzky-Golay smooth reduces noise with minimal distortion of the measured spectra. The presence of electrodes on the skin may induce time dependent changes in impedance spectra. Plots of smoothed and raw data showed no obvious trends with time over our measurement intervals. Impedance spectra were obtained at four second intervals for total elapsed times up to 100 s. Analysis of other spectra sets (30 spectra at 4 s intervals per set) show no time sequence affects. Principal component analysis produced an eigenvalue that contained in excess of 98% of the variance. In addition, the eigenvector contributions associated with smaller eigenvectors did not correlate with the time sequence associated with the collection of the analyzed spectra. Thus, this fast measurement protocol constitutes an impedance measurement technique that avoids the problem of electrode induced physiological changes.

Figures 2a and 2b provide a comparison of 2 different Savitzky-Golay smoothed sets of spectra taken at two different tissue sites on the same rat using the 8 electrode array. This illustration was developed as part of a sequence of experiments intended to assess the possible effects arising from anisotropic tissue properties, removal and replacement of the sensing array, and changing the location of the measurements. In this study spectra were acquired 4 s apart. The 24 spectra shown in Figure 2a were acquired without applicator rotations. At the tissue site for Figure 2b, after acquiring 4 spectra, the applicator was rotated and 4 additional spectra acquired at five additional angles (45, 90, 135 and 180 degrees and then returned to the 90 degree position) for a total of 24 spectra obtained for that target tissue. The heavy lines emphasize the mean spectra for the 24 spectra taken at each tissue site. Plots are typical of spectra obtained from all multiple orientation measurement experiments with any of the three tissue models. Visual inspection indicates very similar

Table 1. Summary of 24 impedance spectra obtained from four separate tissue sites.

	$R \times 10^3$ (SD)	$X \times 10^4$ (sd)	$Y \times 10^4$ (sd)	$A_i \times 10^5$	(sd) $\times 10^5$
Site 1	9.07 (0.72)	1.00 (0.067)	- 0.043 (0.046)	-0.20 0.10 178.4	0.0140 0.0090 9.79
Site 2	9.08 (0.48)	1.00 (0.046)	- 0.047 (0.035)	- 0.20 0.01 185.7	0.0091 0.0071 6.94
Site 3	8.74 (0.54)	0.97	- 0.062	- 0.19 0.01 182.3	0.0100 0.0071 4.77
Site 4	8.80 (0.46)	0.97	- 0.060	- 0.20 0.01 182.7	0.0085 0.0078 9.21
Plate	7.54 (0.48)	0.92	- 0.030	- 0.19 0.03 303.2	0.0087 0.0090 9.86

Site locations with corresponding animal model are reported in the material section. The radius, R, at Site 1 was $9.07x10^3$ with a standard deviation (sd) of 0.72. The fitting model to determine the Nyquist related plot fit was; $X^2 + Y^2 + A_1X + A_2Y + A_3 = 0$.
The plot fit for Site 1 was: $(1x10^4)^2 + (-0.043x10^4)^2 + (-0.2x10^5)(1x10^4) + (0.1x10^5)(-0.043\ x10^4) + (178.4x10^4) = 0$.

spectral results. In order to conduct a quantitative comparison of spectra taken at multiple sites the circular nature of the Nyquist plots was exploited to make a more quantitative evaluation.

Table 1 provides the circle fitting equation; the derived parameter values for the mean spectra (mean of 24) at two different sites are shown in Figures 3a and 3b. These fits provide a convenient method for assessment of the effects of rotating and translating the electrodes. The spectra were fitted individually and the locations of the circle center and radius were recorded. The mean radius and standard deviations from the 24 fits were estimated for each site, along with the mean and standard deviation for the parameters in the polynomial which were used for the fitting process. Table 1 presents these results for the parallel plate application site and the four sites that used the non-penetrating array applicator. Note that the tabular values involve different powers of 10 indicated at the top of each column. The Figure indicates the typical close match to the fitting circle while the table indicates the variability in radius and center location over the spectra used to calculate the mean used for the circle fit. The standard deviation values in the (x,y) location of the model circle centers for tissue site 1 and site 2 reported in Table 1 are (0.067) and (0.046), respectively, for the x-axis locations at both at 1.0 and (0.046) and (0.035), respectively, for the y-axis locations at -0.043 and -0.047. The real axis (x-axis) center locations are reproducible across the four sites and the imaginary y-axis behavior suggests that the circle center is located very near to the real axis.

The deviations for all other x-axis location values and y-axis locations were the same magnitude as the deviations reported for tissue site 1 and 2. Thus, although other investigators [13] have noted that the SC does not yield circular arc Nyquist plots, examination of our data showed deviations from circularity are present, but it still provides a reasonable approach to summarizing the reproducibility of spectral behaviors.

The combination of visual information in Figure 2 and model information from Figure 3 with their corresponding entries in Table 1 provide an assessment of the robustness of the measurements at a target tissue site with respect to removal and replacement of the array accompanied by rotations. It would be expected that translational changes in the position of the model circles and their corresponding radii may appear if the electrode-skin interface was significantly

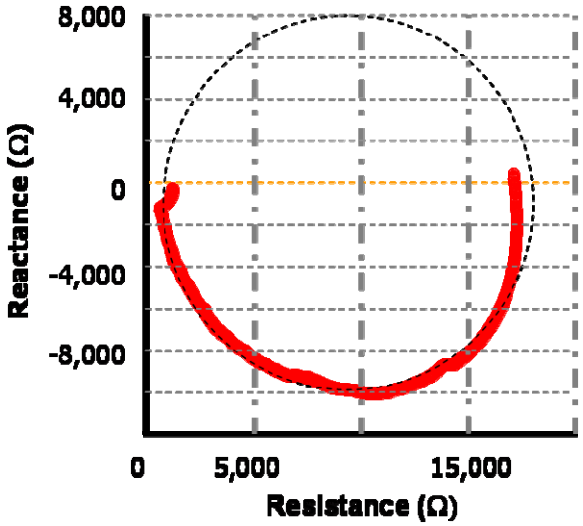

(a)

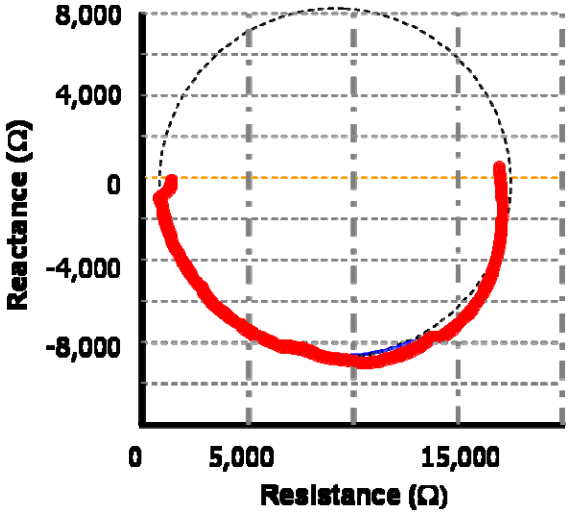

(b)

Figure 4. Typical model fit for 24 specrtra results for the two non-penetrating surface contact applicator, nub, configurations. (a) Mouse tissue spectra using the two column 8 nub electrode applicator (4 electrodes per column) connected to the CythorLab. (b) Rat tissue spectra model using the two column 16 nub electrode applicator (4 electrodes per column) with the outer 4 electrodes columns connected to the CythorLab. The two interior columns (4 electrodes per column) were electrically floating.

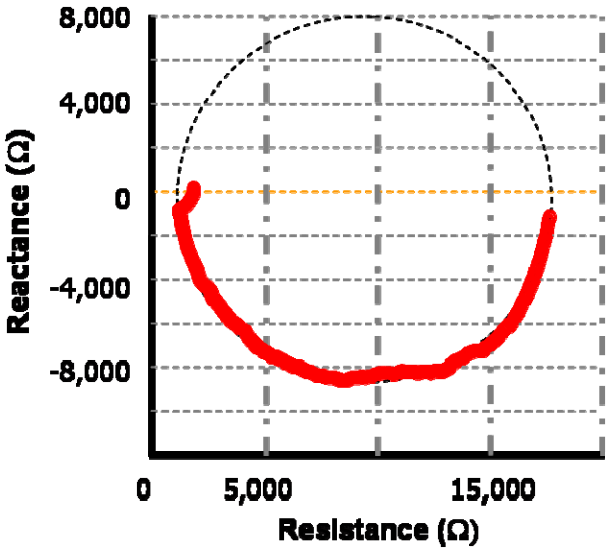

(a)

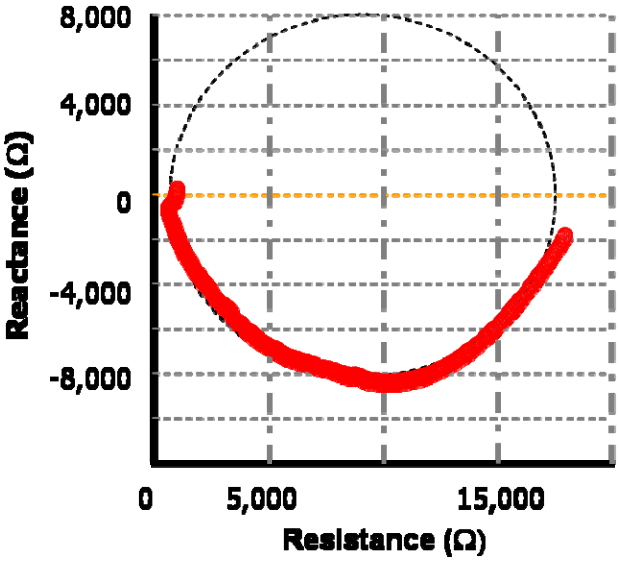

(b)

Figure 5. (a) Typical model fit for 24 spectra results obtained at a site on one animal and (b) show results obtained for the same site on another animal. Both of these spectra were obtained with the parallel plate applicator.

different as a consequence of the removal/rotation/ replacement actions which are incurred in an electroporation procedure. Similar experimental results were observed for the applicator geometries and configurations used in this study with the exception of the concentric electrode device.

Experiments were designed and executed to explore the effects of different applicator configurations and geometries. The differing contact areas, electrode separations and surfaces might affect the resistance and capacitance seen in the analysis and we were concerned with the possibility of introducing new phenomena within the spectra which might make it difficult to extract a feature to be used for an impedance characterization. If an applicator did affect the

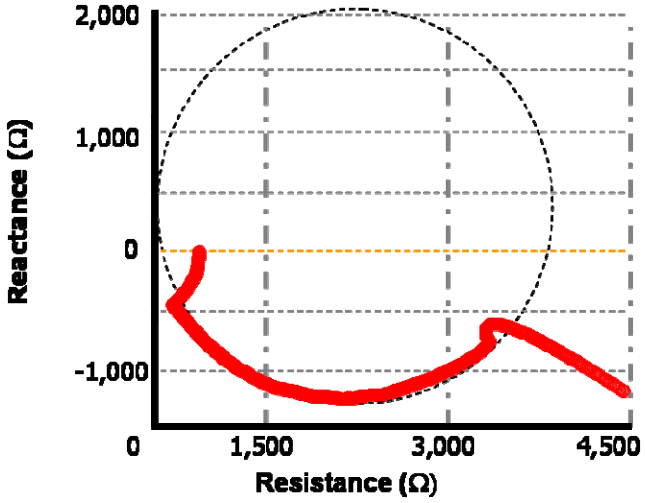

Figure 6. Results from 24 spectra taken 4 s apart using the coaxial applicator on rat tissue. This Figure provides a visual reference for low frequency excursion as the single most striking occasional variation to the typical shapes observed as represented in Figures 3, 4 and 5.

measurement, there might be geometric restrictions on the design of a sensing array if an impedance measurement and/or feedback feature is to be incorporated in a skin target electroporation protocol for a clinical environment. Experiments were carried out on the electrode systems described in the methods/materials sections. Figures 4a and 4b show results for two configurations of the non-penetrating surface point applicator. Figures 5a and 5b show results for two sets of experiments using the parallel plate array.

Figure 6 shows results from experiments using the semicircular array. Again multiple spectra were acquired on each occasion. As expected from the greater contact area the overall impedances are considerably lower than those from the point contact arrays. The low frequency portion of this Nyquist plot indicates a linear excursion towards negative imaginary values even though the higher frequency segment still exhibits the circular characteristic. The reproducibility at a given site for this system is at least comparable to the other arrays studied but it is extremely sensitive to the removal, replacement and site-to-site translation activities. The geometry is such that when the radius of curvature of the target animal tissue zone is small then the external circular electrode of these dimensions has contact problems. These contact problems occurred with the animal models used. Although circle fitting is probably inappropriate in this case, Figure 6 is provided to illustrate the nature of the high frequency circular response and the extent of the low frequency linear excursion. This represents data taken in replicate at a single site with no rotation or replacement. Movements of this kind produced changes in the spectra although the general shapes remained similar.

As would be expected, the significance of this systematic examination of the impedance of tissue rests in the determination of the consistence in the behavior of tissue before, during and after electroporation. If the success of an

electroporation event could be reliably foreshadowed or monitored optional transport conditions for gene transport in cells should be possible.

4 CONCLUSIONS

This circular behavior in the impedance signatures acquired in this study tends to confirm that the measurement system frequency response involves the layers deeper than the SC. This was also suggested by our 2D vertical finite element model studies of field patterns for the arrays not presented here. Both these results provide a reassurance that a non-penetrating skin impedance measurement system will provide impedance profiles of the target tissue at a depth within that tissue where a meaningful electroporation event occurs. The impedances were measured using mice, rats, and guinea pigs as the preliminary part of investigations on the other facets of this work. No phenomena were encountered to suggest that site and subject variation presents any particular difficulty in measurement or any unusual impedance phenomena. No noticeable impact on the impedance signature was detected because of the practice of letting unused electrodes float. However, since such confirmations are used in our clinical trials and the ultimate objective is to develop a measurement system and protocol that uses electroporation applicators as the impedance measurement electrodes, the question was not if there was no effect but if the effect prevented using these applicator configurations as sensing electrodes.

The arrays that contained gold coated hemispherical electrodes in this study are currently incorporated in successful delivery experiments and the robust behavior observed in our impedance measurements suggests that there are no major obstacles to their deployment as a monitoring component. The inevitable noise issues have been addressed along with the problems associated with time dependent physiological responses to the presence of the electrodes. Preliminary calculations suggest that a scale free characteristic feature can be extracted. The feature extraction process developed from these studies is an interim version which may be modified by observations of post injection and post electroporation spectra to define the data trajectory which identifies a successful electroporation. From this preliminary experimental work we have identified a transformation to a common data space in which the spectral differences are clearly exhibited in a form useful as an index of change. The structures of the spectra show no rapid changes with frequency so that to ease computing requirements they were re-sampled down to about 800 complex data points from the original 16000 plus points.

In addition, we have assembled a small test array of 96 spectra from different experiments and converted them to standard form. This test array included a similar number of spectra for all applicators, tissue models and all 10 measurement sites. A Karhunen-Loeve expansion (principal component analysis) was used to derive a description of the 96 spectra in terms of two or three component vectors depending on the sensitivity requirements. These vectors were carried over to examine the behavior of a small set of post injection spectra and were found to be useful measures for the time dependent changes which occur after injection of the drug/gene carrying media. Work on the effect of the injection of the drug/gene carrying media has been extended along with electroporation studies.

In summary, the value of incorporating impedance spectroscopy as a measurement tool for *in vivo* electroporation is obvious. If the success of the electroporation event could be monitored as the treatment progresses, the success of the transport of the gene through the cell membrane could be established. In addition, if it becomes certain that electroporation has occurred, the electroporation signature could be altered and applied to the electroporated tissue to optimize the transport of the gene into the cells. At this point, we have established that it is not necessary to obtain pre-injection spectra nor does the manipulations of equipment using arrays of the kind examined have any significant effect on the impedance measurements. These arrays are already in use as electroporation devices so that the monitoring process may incorporate their use. In the event of new or alternative configuration applicators moving into the clinical arena, there is a high likelihood that they also can be used for measurement signal and electroporation signature delivery. In any event, the techniques developed in this study will permit a quantitative assessment of such applicators impact on the tissue.

ACKNOWLEDGMENT

The authors would like to thank the University of South Florida Center for Molecular Delivery, Tampa, FL. Additionally, R. J. Connolly and J. I. Rey would like to thank NSF IGERT (DGE-0221681) and Florida Center of Excellence for Biomolecular Identification and Targeted Therapeutics programs for their support.

REFERENCES

[1] M. Jaroszeski, R. Gilbert, C. Nicolau, and R. Heller, “In-vivo gene delivery by electroporation”, Advanced Drug Delivery, Vol. 35, pp. 131–137, 1999.

[2] D. Cukjati, D. Batiuskaite, F. Andre, D. Miklavcic, and L. M. Mir, “Real time electroporation control for accurate and safe in vivo non-viral gene therapy”, Bioelectrochemistry, Vol. 70, pp. 501–507, 2007.

[3] G. Widera, M. Austin, D. Rabussay, C. Goldbeck, S. W. Barnett, M. Chen, L. Leung, G. R. Otten, K. Thudium, M. J. Selby, and J. B. Ulmer, “Increased DNA vaccine delivery and immunogenicity by electroporation in vivo”, J. Immunology, Vol. 164, pp. 4635–4640, 2000.

[4] L. C. Heller, M. J. Jaroszeski, D. Coppola, A. N. McCray, J. Hickey, and R. Heller, “Optimization of cutaneous electrically mediated plasmid DNA delivery using novel electrode”, Gene Therapy, Vol. 14, pp. 275–280, 2007.

[5] L. A. Hirao, L. Wu, A. S. Khan, A. Satishchandran, R. Draghia-Akli, and D. B. Weiner, “Intradermal/subcutaneous immunization by electroporation improves plasmid vaccine delivery and potency in pigs and rhesus macaques”, Vaccine, Vol. 26, pp. 440–448, 2008.

[6] A. I. Daud, R. C. DeConti, S. Andrews, P. Urbas, A. I. Rikera, V. K. Sondak, P. N. Munster, D. M. Sullivana, K. E. Ugen, J. L. Messina, and R. Heller, "Phase I trial of interleukin-12 plasmid electroporation in patients with metastatic melanoma", J. Clinical Oncology, Vol. 26, pp. 5896–5903, 2008.

[7] M. L. Lucas and R. Heller, "Il-12 gene therapy using an electrically mediated nonviral approach reduces metastatic growth of melanoma", DNA and Cell Biology, Vol. 22, pp. 755–763, 2003.

[8] L. C. Heller and R. Heller, "In vivo electroporation for gene therapy", Human Gene Therapy, vol. 17, pp. 890–897, 2006.

[9] R. Gilbert, M. J. Jaroszeski, L. Heller, and R. Heller, "Electric field enhanced plasmid delivery to liver hepatocellular carcinomas", Technology in Cancer Research and Treatment, Vol. 1, pp. 355–364, 2002.

[10] R. V. Davalos, B. Rubinsky, and D. M. Otten, "A feasibility study for electrical impedance tomography as a means to monitor tissue electroporation for molecular medicine", IEEE Trans. Biomedical Engineering, Vol. 49, pp. 400–403, 2002.

[11] S. Grimnes, "Impedance measurement of individual skin surface electrodes", Medical and Biological Engineering and Computing, Vol. 21, pp. 750–755, 1983.

[12] K. A. Holbrook and G. F. Odland, "Regional differences in the thickness (cell layers) of the human stratum corneum: an ultrastructural analysis," *Journal of Investigative Dermatology*, vol. 62, pp. 415–422, 1974.

[13] T. Yamamoto and Y. Yamamoto, "Electrical properties of the stratum corneum", Medical and Biological Engineering and Computing, Vol. 14, pp. 592–594, 1976.

[14] J. Glahder, B. Norrild, M. B. Persson, and B. R. Persson, "Transfection of HeLa-cells with pEGFP plasmid by impedance power assisted electroporation", Biotechnology and Bioengineering, Vol. 92, pp. 267–276, 2005.

[15] R. Gilbert, M. Jaroszeski, and R. Heller, "Novel electrode designs for electrochemotherapy", Biochimia et Biophysica Acta, Vol. 1334, pp. 9–14, 1997.

[16] L. F. Glass, N. A. Fenske, J. M. J., R. Perrott, D. T. Harvey, D. S. Reintgen, and R. Heller, "Bleomycin-mediated electrochemotherapy of basal cell carcinoma", J. American Academy of Dermatology, Vol. 34, pp. 82–86, 1996.